ESC HEART FAILURE
ESC Heart Failure 2020; **7**: 3075–3085
Published online 4 August 2020 in Wiley Online Library (wileyonlinelibrary.com) **DOI:** 10.1002/ehf2.12935

ORIGINAL RESEARCH ARTICLE

Prediction of haemodynamics after interatrial shunt for heart failure using the generalized circulatory equilibrium

Takuya Nishikawa[1,2], Keita Saku[1,2]*, Kiyoshi Uike[3], Kazunori Uemura[1], Genya Sunagawa[2], Takeshi Tohyama[2], Keimei Yoshida[2], Takuya Kishi[4], Kenji Sunagawa[5] and Hiroyuki Tsutsui[2]

[1]*Department of Cardiovascular Dynamics, National Cerebral and Cardiovascular Center, 6-1 Kishibe-Shimmachi, Suita, Osaka, Japan;* [2]*Department of Cardiovascular Medicine, Graduate School of Medical Sciences, Kyushu University, Fukuoka, Japan;* [3]*Department of Pediatrics, Graduate School of Medical Sciences, Kyushu University, Fukuoka, Japan;* [4]*Department of Fukuoka Health and Welfare Sciences, International University of Health and Welfare, Okawa, Japan;* [5]*Circulatory System Research Foundation, Fukuoka, Japan*

Abstract

Aims Interatrial shunting (IAS) reduces left atrial pressure in patients with heart failure. Several clinical trials reported that IAS improved the New York Heart Association score and exercise capacity. However, its effects on haemodynamics vary depending on shunt size, cardiovascular properties, and stressed blood volume. To maximize the benefit of IAS, quantitative prediction of haemodynamics under IAS in individual patients is essential. The generalized circulatory equilibrium framework determines circulatory equilibrium as the intersection of the cardiac output curve and the venous return surface. By incorporating IAS into the framework, we predict the impact of IAS on haemodynamics.

Methods and results In seven mongrel dogs, we ligated the left anterior descending artery and created impaired cardiac function with elevated left atrial pressure (baseline: 7.8 ± 1.0 vs. impaired: 11.9 ± 3.2 mmHg). We established extracorporeal left-to-right atrial shunting with a centrifugal pump. After recording pre-IAS haemodynamics, we changed IAS flow stepwise to various levels and measured haemodynamics under IAS. To predict the impact of IAS on haemodynamics, we modelled the fluid mechanics of IAS by Newton's second law and incorporated IAS into the generalized circulatory equilibrium framework. Using pre-IAS haemodynamic data obtained from the dogs, we predicted the impact of IAS flow on haemodynamics under IAS condition using a set of equations. We compared the predicted haemodynamic data with those measured. The predicted pulmonary flow [r^2 = 0.88, root mean squared error (RMSE) 11.4 mL/min/kg, $P < 0.001$), systemic flow (r^2 = 0.92, RMSE 11.2 mL/min/kg, $P < 0.001$), right atrial pressure (r^2 = 0.92, RMSE 0.71 mmHg, $P < 0.001$), and left atrial pressure (r^2 = 0.83, RMSE 0.95 mmHg, $P < 0.001$) matched well with those measured under normal and impaired cardiac function. Using this framework, we further performed a simulation study to examine the haemodynamic benefit of IAS in heart failure with preserved ejection fraction. We simulated the IAS haemodynamics under volume loading and exercise conditions. Volume loading and exercise markedly increased left atrial pressure. IAS size-dependently attenuated the increase in left atrial pressure in both volume loading and exercise. These results indicate that IAS improves volume and exercise intolerance.

Conclusions The framework developed in this study quantitatively predicts the haemodynamic impact of IAS. Simulation study elucidates how IAS improve haemodynamics under volume loading and exercise conditions. Quantitative prediction of IAS haemodynamics would contribute to maximizing the benefit of IAS in patients with heart failure.

Keywords Interatrial shunting; Heart failure; Circulatory equilibrium; Haemodynamics

Received: 5 December 2019; Revised: 13 July 2020; Accepted: 19 July 2020
**Correspondence to: Keita Saku, Department of Cardiovascular Dynamics, National Cerebral and Cardiovascular Center, 6-1 Kishibe-Shimmachi, Suita, Osaka, Japan. Email: saku.keita@ncvc.go.jp*

Introduction

The number of patients with heart failure (HF) is increasing with aging of the population.[1] Regardless of the underlying aetiology of HF, 70–90% of patients with acute decompensated HF present with pulmonary congestion resulting from elevated left atrial pressure (P_{LA}).[2,3] Frequent occurrence of acute decompensated HF leads to progressive deterioration of cardiac function and quality of life, resulting in poor survival outcome.[4] Therefore, we need new strategies to prevent the acute elevation of P_{LA} in patients with HF.

Interatrial shunting (IAS) by transvenous catheter technique has been developed recently.[5–8] IAS translocates blood volume from the pulmonary circulation to the systemic circulation and prevents the acute increase in P_{LA}. The degree of volume translocation depends on the pressure gradient between P_{LA} and right atrial pressure (P_{RA}). The interatrial shunt device system (IASD®), which was developed by Corvia Medical, Inc., is composed of left and right atrial discs (19 mm outer diameter) with an 8 mm communication. In a Phase 2 trial (REDUCE LAP-HF I), Feldman *et al.*[6] reported that IASD® improved the NYHA score, increased the distance of 6 min walk, and attenuated the increase in pulmonary capillary wedge pressure (PCWP) during exercise. In contrast, IAS had little effect on PCWP or systemic flow (Q_S) at rest in patients with HF and preserved ejection fraction (HFpEF). The V-Wave® device (V-Wave Ltd.) with a 5.1 mm inner diameter is designed to prevent right-to-left atrial flow. In a Phase 1 clinical trial, Del Trigo *et al.*[7] reported that the V-Wave® system improved the NYHA score and the distance of 6 min walk in patients with HF and reduced ejection fraction (HFrEF). Because various conditions other than the IAS size, such as right and left cardiac function, vascular properties, and stressed blood volume, may also affect the haemodynamic impact of IAS, the benefit of IAS varies among patients with HF. Wessler *et al.*[8] reported that IASD® suppressed PCWP during exercise to a greater extent in patients with high PCWP at rest than in those with low PCWP. However, we do not have an established method or a single marker that detects responder or non-responder to IAS or indicate the appropriate device size for individual patients with HF. Quantitative prediction of the impact of IAS on haemodynamics is crucial and may allow appropriate selection of patient and device.

Guyton[9] proposed that the intersection of the cardiac output (CO) curve, and the venous return curve represents the circulatory equilibrium. Sunagawa *et al.*[10] extended this framework to include the pulmonary circulation by introducing P_{LA} and representing the CO curves and venous return as a function of P_{RA} and P_{LA}. They derived the analytical representation of the CO curve using the framework of ventricular arterial coupling and the venous return surface using the resistance-compliance distributed circuit (generalized circulatory equilibrium). The generalized circulatory equilibrium enabled us to predict haemodynamics under extracorporeal membrane oxygenation and left ventricular assist device.[11–14]

Using the concept of generalized circulatory equilibrium, we developed a simple framework to predict the impact of IAS on haemodynamics aiming to optimize IAS therapy in individual patients with HF. We validated the framework using a dog model of IAS with graded changes of the left to the right atrial shunt flow.

Methods

Theoretical considerations

Because IAS does not directly change the cardiac function or vascular properties, we consider that IAS haemodynamics can be modelled by simply applying the equation: $Q_{IAS} = Q_P - Q_S$ in generalized circulatory equilibrium, where Q_{IAS} is the shunt flow, Q_P is pulmonary flow, and Q_S is systemic flow.

We derived the integrated CO curves from the left and right CO curves. In the left heart, the CO curve is a simple logarithmic function of P_{LA}[12] as follows:

$$Q_S = S_L[\ln(P_{LA} - F_L) + H_L] \quad (1)$$

where S_L, F_L, and H_L are empirical parameters of the left heart. The values of F_L and H_L used in this study are 2.03 and 0.8, respectively, based on a previous report.[12] In the right heart, the downstream pressure of the pulmonary artery, that is, P_{LA}, is not negligibly small relative to the mean pulmonary arterial pressure. We previously reported that the downstream pressure could be incorporated into the CO curves by the following equation[13,14]:

$$Q_P = S_R[\ln(P_{RA} - F_R) + H_R] - \frac{1 - RVEF_e}{R_p}P_{LA} \quad (2)$$

where S_R, F_R, and H_R are empirical parameters of the right heart, $RVEF_e$ is effective RV ejection fraction, and R_P is pulmonary vascular resistance. In this study, we set F_R = 2.13, H_R = 1.9, and $RVEF_e$ = 0.6 for normal RV function, and R_P = 0.1 mmHg/mL/min/kg for normal pulmonary circulation as reported previously.[12,14,15]

We previously reported that in a distributed resistance-compliance vascular model, the following equations represent the stressed blood volume of the systemic circulation and pulmonary circulation[11]:

$$V_S = W_S Q_S + C_S P_{RA} \quad (3)$$

$$V_P = W_P Q_P + C_P P_{LA} \quad (4)$$

$$V_T = V_S + V_P \quad (5)$$

where V_S, V_P, and V_T are stressed blood volume of systemic circulation, pulmonary circulation, and the sum of the two, respectively. W_S, W_P, C_S, and C_P are vascular parameters, respectively. We set W_S = 0.106 min, W_P = 0.024 min,

C_S = 2.53 mL/mmHg/kg, and C_P = 0.45 mL/mmHg/kg from previous reports.[11,13,15,16]

We used Newton's second law to model the IAS fluid dynamics as follows[17]:

$$Q_{IAS} = Q_P - Q_S \tag{6}$$

$$Q_{IAS} = C_d S_{IAS} \sqrt{\frac{2(P_{LA} - P_{RA})}{\rho}} \tag{7}$$

where Q_{IAS}, C_d, S_{IAS}, and ρ are IAS flow, discharge coefficient, cross-sectional area of IAS, and density of blood, respectively. We set C_d = 0.74 (unitless) and ρ = 1.05 g/cm^3 as reported previously.[17,18] Once we have determined S_L, S_R, and V_T, we can predict IAS haemodynamics by simultaneously solving these seven equations. Details of the calculation are given in the Supporting Information.

Animal preparation

We used seven adult mongrel dogs weighing 14.3–17.9 kg. The investigation conforms to the Guide for the Care and Use of Laboratory Animals published by the US National Institutes of Health (NIH Publication No. 85-23, revised 1985). The Committee on Ethics of Animal Experiments at Kyushu University Graduate School of Medical Sciences approved the experiments.

We induced anaesthesia with intravenous pentobarbital sodium (25 mg/kg) and pancuronium bromide (0.08 mg/kg), performed endotracheal intubation, and maintained an appropriate anaesthesia level during the experiment by continuous infusion of isoflurane (1–2%). We kept body temperature between 37°C and 38°C. We bilaterally denervated the carotid sinuses and vagotomised to abolish the neural reflexes including baroreflex. We inserted a 5Fr sheath into the right femoral artery to measure arterial pressure (AP). We inserted a high-fidelity micromanometer (Millar Instruments, Houston, TX) into LV through the free wall. We inserted a pair of draining cannula and fluid-filled catheters each into the left (LA) and right atria (RA). We connected the fluid-filled catheters to pressure transducers (model DX-360; Nihonkohden, Tokyo, Japan) to measure P_{LA} and P_{RA}. We connected the two cannulas via a centrifugal pump (CBBPX-80; Medtronic, Minneapolis, MN) to mimic IAS and mounted an in-line ultrasonic flowmeter (model XL; Transonics, Ithaca, NY) in the circuit to measure Q_{IAS} continuously. We also placed an ultrasonic flowmeter (model PSB; Transonic, Ithaca, NY) around the ascending aorta to measure Q_S (Supporting Information, *Figure S1*). We estimated Q_P as the sum of Q_S and Q_{IAS} ($Q_P = Q_{IAS} + Q_S$).

Experimental protocols

Under normal conditions, we first clamped the shunt circuit (Q_{IAS} = 0) and recorded baseline Q_S, Q_P, P_{LA}, and P_{RA} (*Figure 1*). Using the baseline haemodynamic data, we estimated S_L, S_R, and V_T from equations 1–5. We changed Q_{IAS} stepwise to vary the ratio of the pressure gradient between P_{LA} and P_{RA}, to Q_{IAS} at 90, 60, 30, and 10 × 10^{-3} mmHg/mL/min/kg. In each step, after waiting for 1 min, we recorded Q_S, Q_{IAS}, P_{LA}, and P_{RA} for 10 s. Because we created an artificial shunt, we estimated effective S_{IAS} from Q_{IAS} and the pressure gradient between P_{LA} and P_{RA} using equation 7. We predicted Q_S, Q_P, P_{LA}, and P_{RA} from S_L, S_R, V_T, and S_{IAS} and compared the predicted values with those measured.

After the experiment in the normal heart condition, we ligated the left anterior descending artery to create impaired cardiac function. One hour after the left anterior descending artery ligation, we repeated the same protocol as described above.

Computational simulation

Flash pulmonary oedema is a cardinal feature of HFpEF and is caused by an acute increase of P_{LA} after volume loading or exercise.[19,20] HFpEF may be a good indication for IAS intervention because IAS prevents the acute increase in P_{LA}. To elucidate the haemodynamic benefits of IAS in HFpEF patients, we performed a computational simulation study of haemodynamics with IAS under volume loading and exercise conditions in HFpEF patients using the proposed framework.

We determined the haemodynamic parameters of HFpEF patients based on previous reports as follows. Maeder *et al.*[21] and Kaye *et al.*[22] simulated exercise haemodynamics with IAS using a multi-factor haemodynamic model. To determine the CO curve, we used the following equation that we reported previously.[12,23]

$$CO = \frac{1}{k}\frac{E_{es}}{\frac{E_{es}}{HR} + R}\left(\ln(P_a - F) + H\right) \tag{8}$$

where E_{es}, HR, R, P_a, are end-systolic elastance of ventricles, heart rate, resistance, and atrial pressure of systemic or pulmonary circulation, respectively; k is the stiffness component of the ventricle. F and H are constants of the CO curve. We used equations 3–5 to determine the venous return surface. First, we determined E_{es}, R, and HR based on the simulation report of Kaye *et al.*[22] We set F to 0 to simplify the equation. The remaining parameters, that is, k, H, W, and C, were determined to reproduce the haemodynamics according to previous reports.[21,22]

To simulate the exercise condition based on the report of Kaye *et al.*,[22] we increased E_{es}, heart rate and stressed volume; decreased resistance; and assumed the exercise

FIGURE 1 Experimental design to verify the accuracy of haemodynamic prediction. We determined S_L, S_R, and total stressed blood volume (V_T) under baseline conditions. Then, we changed Q_{IAS} and determined S_{IAS} from the left and right atrial pressure gradient and shunt flow (Q_{IAS}). We predicted pulmonary flow (Q_P), systemic flow (Q_S), right atrial pressure (P_{RA}), and left atrial pressure (P_{LA}) using the framework and compared the predicted values with measured. S_L and S_R are slopes of cardiac output (CO) curves; F_L, H_L, F_R, and H_R are empirical parameters of the left and right heart; W_S, W_P, C_S, and C_P are vascular parameters. C_d, discharge coefficient; R_P, pulmonary vascular resistance; $RVEF_e$, effective right ventricular ejection fraction; S_{IAS}, functional cross-sectional area of interatrial shunt (IAS); V_P, pulmonary stressed blood volume; V_S, systemic stressed blood volume; V_T, total stressed blood volume; ρ, the density of blood.

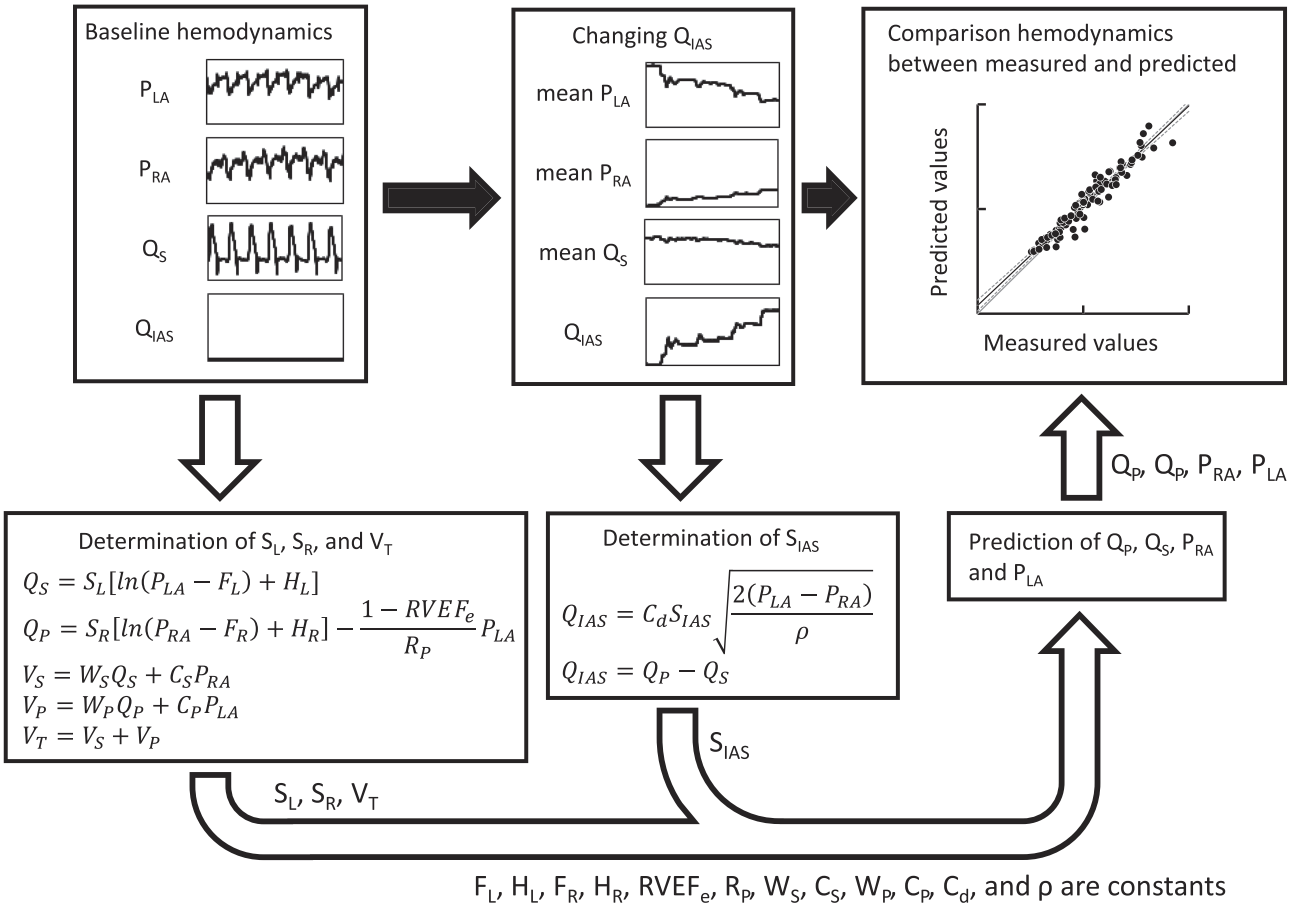

intensity to be 0.63 W/kg, which was the limiting exercise intensity.[21] We changed these parameters (E_{es}, heart rate, stressed volume, and resistance) linearly from 0 to 1 W/kg work rate. Details of the simulation parameters are given in the Supporting Information.

Protocol for the simulation study

In the volume loading simulation, we set baseline Q_S at 5.3 L/min by changing stressed blood volume for various shunt sizes ranging from 0 to 20 mm in diameter. We then loaded blood volume until 1000 mL. In the exercise simulation, we set the same baseline as the volume loading simulation and changed exercise-related parameters according to the work rate from 0 to 1 W/kg.

Data analysis

We digitized all data at 200 Hz using a 16-bit analogue to digital converter (Power Lab 16/35; ADInstruments, NSW, Australia) and stored in a dedicated laboratory computer system. We averaged digitized data over 10 s when time-series data reached a steady state.

Statistical analysis

We expressed data as mean ± SD and used paired *t*-test to compare haemodynamics before and after the left anterior descending artery ligation. Repeated measures ANOVA was used for comparison of haemodynamic data under various IAS conditions. Differences were considered significant at $P < 0.05$. We performed the statistical analysis using R

version 3.4.3 (R Foundation for Statistical Computing, Vienna, Austria).

Results

Creation of impaired cardiac function in dogs

Table 1 shows haemodynamics before (Normal) and after induced myocardial infarction (Impaired). We determined S_L, S_R, and V_T using haemodynamic data under Normal and Impaired conditions. Myocardial infarction significantly increased P_{LA} and P_{RA} and decreased S_L. In contrast, myocardial infarction did not change S_R significantly. V_T remained unchanged irrespective of the induction of myocardial infarction.

Prediction of IAS haemodynamics

Figure 2 shows the representative time series of IAS haemodynamics. Increases in Q_{IAS} decreased AP, P_{LA}, and Q_S, but increased P_{RA}. At maximum Q_{IAS} [$(P_{LA} - P_{RA})/Q_{IAS} = 10 \times 10^{-3}$ mmHg/mL/min/kg], the pressure difference between P_{LA} and P_{RA} was <1 mmHg. Haemodynamic data during IAS are summarized in Supporting Information, *Table S1*. As described in the Methods section, we determined S_L, S_R, and V_T and predicted haemodynamics at various levels of IAS flow. *Figure 3* demonstrates the relationship between predicted and measured Q_P, Q_S, P_{RA}, and P_{LA}. The narrow error distributions and 95% confidence intervals show reasonable accuracy of the proposed framework.

Computational simulation study

Illustrated in *Figure 4* is the simulated IAS haemodynamics during acute volume loading in HFpEF. Volume loading markedly increased venous pressures (P_{RA} and P_{LA}) (*Figure 4C* and *D*) but marginally increased CO (Q_P and Q_S) (*Figure 4A* and *B*), illustrating volume intolerance in HFpEF patients. IAS size-dependently attenuated the increase in P_{LA} (*Figure 4D*), implying that IAS improves volume tolerance at the expense of increased P_{RA} (*Figure 4C*) and Q_P (*Figure 4A*). The P_{LA}-suppressing effect diminished when the IAS size was 8 mm or larger (*Figure 4E*).

Figure 5 illustrates the simulated IAS haemodynamics during exercise in HFpEF. As in the case of volume loading, IAS attenuated the increase in P_{LA} (*Figure 5D* and *E*). Exercise-induced increases in E_{es} and heart rate and decrease in resistance could lower P_{LA}. However, exercise-induced increase in stressed volume counteracts these P_{LA}-lowering effects and increases P_{LA}. These results imply that volume intolerance of HFpEF leads to an increase in P_{LA} during exercise.

Table 1 Haemodynamics under normal and impaired left ventricular function

	Normal	Impaired
AP (mmHg)	119.3 ± 25.8	126.2 ± 21.0
HR (b.p.m.)	147.9 ± 23.7	141.6 ± 18.5
P_{LA} (mmHg)	7.8 ± 1.0	11.9 ± 3.2*
P_{RA} (mmHg)	5.5 ± 1.0	6.4 ± 1.2*
CO (mL/min/kg)	100.6 ± 30.0	89.3 ± 35.9
Predicted S_L (mL/min/kg)	50.0 ± 17.7	37.0 ± 16.6*
Predicted S_R (mL/min/kg)	80.0 ± 26.2	77.9 ± 32.1
Predicted V_T (mL/kg)	30.5 ± 2.5	33.0 ± 2.6

Data are expressed as mean ± SD. S_L and S_R are parameters of the logarithmic function for left and right hearts, respectively. AP, arterial pressure; CO, cardiac output; HR, heart rate; P_{LA}, left atrial pressure; P_{RA}, right atrial pressure; V_T, total stressed blood volume.
*$P < 0.05$.

FIGURE 2 Representative time series data of interatrial shunt (IAS) haemodynamics. We increased IAS flow (Q_{IAS}) stepwise by changing the speed of the centrifugal pump. The increase in IAS flow decreases arterial pressure (AP), left atrial pressure (P_{LA}), and systemic flow (Q_S), but increases right atrial pressure (P_{RA}).

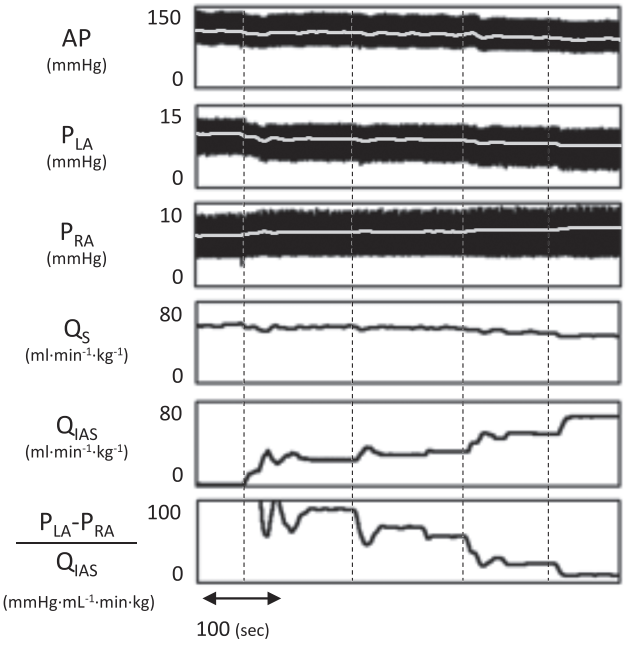

Discussions

In this study, we proposed a framework to predict the haemodynamic impact of IAS. In a dog model of IAS, the framework predicted haemodynamics under various IAS flow rates reasonably well in both normal and impaired cardiac

FIGURE 3 Accuracy of prediction. Top panels show the relation between predicted and measured values for pulmonary flow (Q_P), systemic flow (Q_S), left atrial pressure (P_{LA}), and right atrial pressure (P_{RA}). Twenty-eight data sets obtained from six dogs were plotted. Bland–Altman plots (bottom) show acceptable agreement. Open circles and filled circles represent haemodynamics under normal and impaired cardiac function, respectively. Solid lines and dashed lines represent the regression lines and 95% confidence intervals, respectively. r^2, coefficient of determination; RMSE, root mean squared error; LOA, limit of agreement (mean ± 1.96 SD).

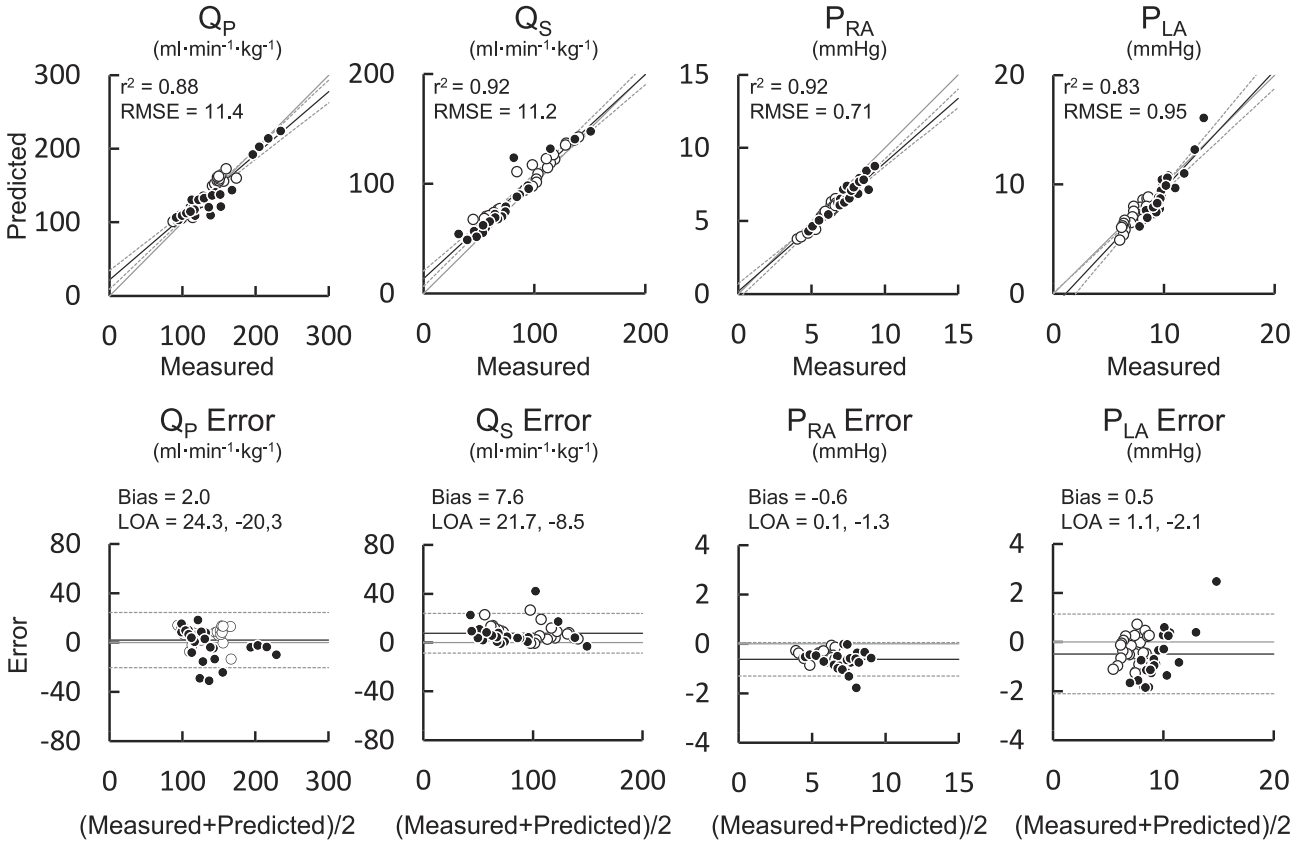

function. Computational simulation study indicated that IAS below 20 mm in diameter size-dependently attenuated the increase in P_{LA} in both volume loading and exercise loading under the HFpEF conditions.

Prediction of interatrial shunting haemodynamics by generalized circulatory equilibrium

In theory, IAS does not alter S_R, S_L, pumping ability of the heart, V_T, or total stressed blood volume. However, IAS translocates the stressed blood volume from the pulmonary to the systemic circulation, depending on the pressure gradient between the right and left atria as well as IAS size. Thus, we modelled IAS haemodynamics by the shunt flow from the systemic circulation to the pulmonary circulation ($Q_{IAS} = Q_P - Q_S$) in generalized circulatory equilibrium. As shown in *Figure 3*, the proposed framework can predict IAS haemodynamics under various shunt flow rates irrespective of cardiac function. It is well known that the generalized circulatory equilibrium accurately describes the overall integrated haemodynamics, which is defined by the pressure and flow of the right and left heart. Once we established the model using haemodynamic parameters in a given condition, we could predict haemodynamics under various conditions such as myocardial infarction, blood volume gain and/or loss, extra-corporeal membrane oxygenation, and left ventricular assist device.[12–14] The results of this study also support the robustness of generalized circulatory equilibrium.

Except for severe HF, Q_S hardly decreases because the oxygen demand of the whole body determines Q_S. Therefore, the presence of IAS may not reduce Q_S or P_{LA} at rest. In contrast, IAS attenuates the P_{LA} elevation against the increase of venous return to the left atrium. Because the slope of the CO curve is much steeper in the right ventricle than the left ventricle, the increase in P_{RA} by IAS may be small compared with the decrease in P_{LA}.

FIGURE 4 Volume loading simulation. Baseline stressed volume is set at systemic flow (Q_S) = 5.3 L/min for several interatrial shunt (IAS) sizes. The *x*-axis shows the loading volume. The *y*-axis shows IAS size. Volume loading increases pulmonary flow (Q_P) (A), Q_S (B), right atrial pressure (P_{RA}) (C), and left atrial pressure (P_{LA}) (D). The relationship between P_{LA} and IAS size under volume load of 0, 500, and 1000 mL (E). Dotted lines, broken lines, and solid lines represent 0, 500, and 1000 mL of loading volume, respectively. IAS significantly antagonizes the increase in P_{LA} in a size-dependent manner.

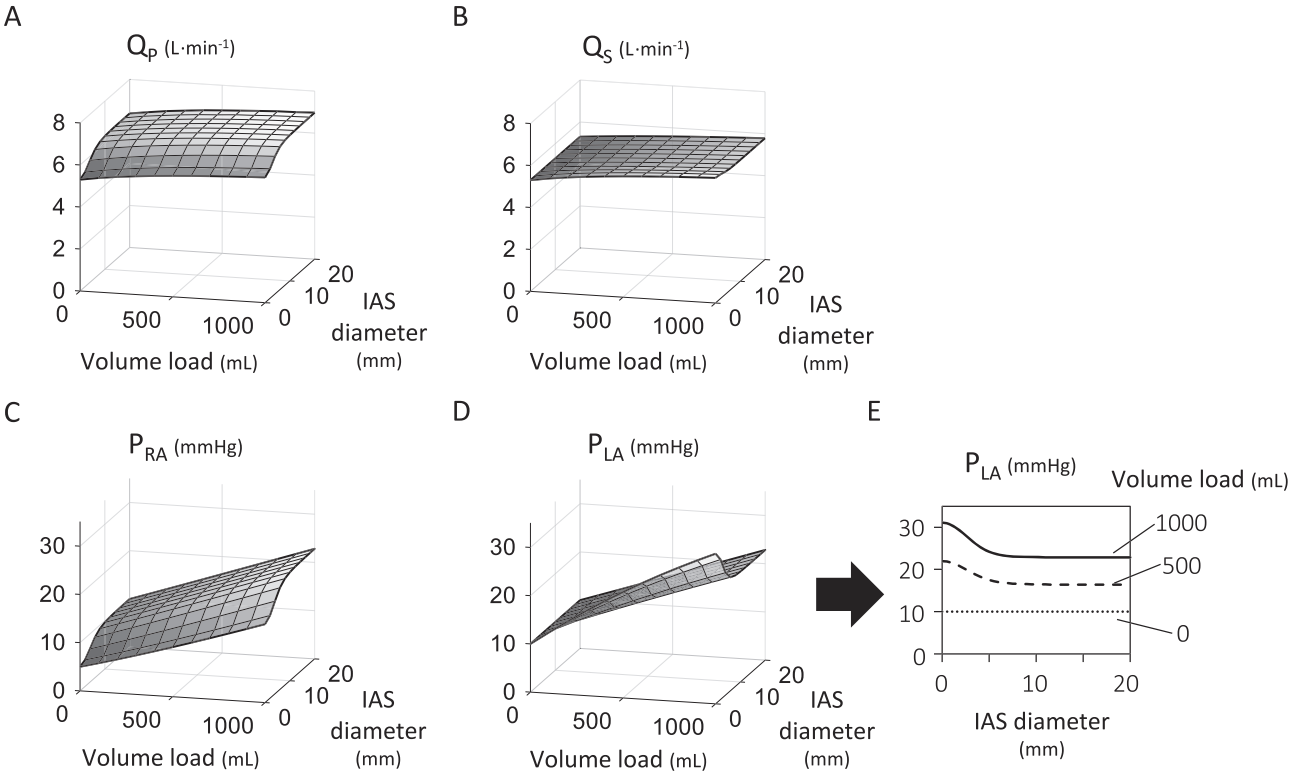

Real-world validation

In order to validate the clinical feasibility of our proposed framework, we applied the data from the REDUCE LAP-HF I trial[6,8] to our framework and compared the predicted values with those measured. To apply the clinical data to the simulation, we had to incorporate some assumptions into the framework. P_{RA} and P_{LA} were substituted by central venous pressure (CVP) and PCWP, respectively. C_d for clinical IAS was calculated from post-IAS pressure gradient (PCWP-CVP), Q_{IAS}, and equation 7 in the theoretical considerations section. We also assumed patients' height to be 170 cm and adjusted the body weight to match the mean BMI in the original data.[8]

We predicted post-IAS haemodynamics using baseline haemodynamics [CO, PCWP, CVP, systemic vascular resistance (R_S), and R_P]. As shown in *Table 2* (constant V_T), we succeeded to predict the trend of haemodynamic changes after IAS. The predicted arterial pressure (AP), Q_S, and P_{LA} are lower than those measured at 6 months after IAS. Because our proposed framework predicts acute haemodynamic change after IAS, altered V_T in the chronic phase may contribute greatly to those differences. Considering this possibility, we adjusted post-IAS V_T so that mean post-IAS AP equalled that at baseline (adjusted V) and obtained better prediction of haemodynamics.

Optimization of interatrial shunting for clinical application

We predicted post-IAS haemodynamics using pre-IAS CO, P_{LA}, and P_{RA}. Because these parameters are generally available in clinical settings, we can predict post-IAS haemodynamics in each patient. It is well known that responders and non-responders to IAS therapy exist because several cardiovascular properties determine the impact of IAS on haemodynamics. In addition, recent device development has allowed selection of several sizes of IAS. Because the IAS size also affects the degree of PCWP and systemic CO reduction, we need to choose the optimal device size according to cardiovascular properties, volume status, and body size in an individual patient with HF. The framework that we developed makes it possible to predict the haemodynamics after IAS and assess patient-specific haemodynamic risks such as post-IAS low CO, high pulmonary flow causing pulmonary

DOI: 10.1002/ehf2.12935

FIGURE 5 Exercise simulation studies. We adjusted baseline stressed volume so that systemic flow (Q_S) was 5.3 L/min regardless of interatrial shunt (IAS) size. The *x*-axis shows exercise intensity. The *y*-axis shows the intra-atrial shunt (IAS) size. Exercise increases pulmonary flow (Q_P), Q_S, right atrial pressure (P_{RA}), and left atrial pressure (P_{LA}). The relationship between P_{LA} and IAS size under the exercise load of 0, 0.5, and 1 W/kg (E). The dotted line, broken line, and solid line represent 0, 0.5, and 1 W/kg of exercise intensity, respectively. IAS significantly attenuates the increase in P_{LA} in a size-dependent manner.

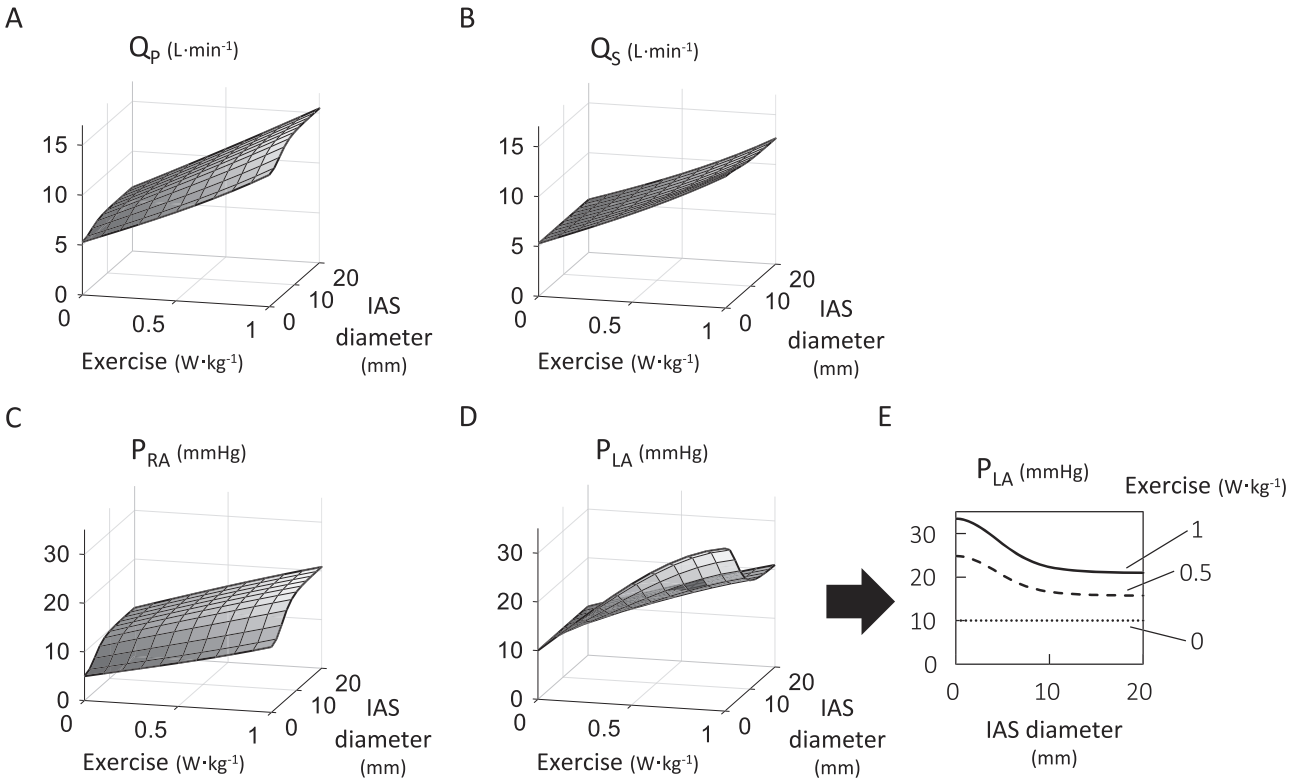

hypertension, and worsening of right HF, which contributes to the selection of patient and IAS size.

Kaya *et al.*[22] reported exercise haemodynamics in the presence of IAS using a multi-element haemodynamic model. Because they adjusted model parameters from human mass haemodynamic data, they did not address haemodynamic simulation in individual patients. Our proposed framework that allows prediction of patient-specific post-IAS haemodynamics using pre-IAS haemodynamic data is potentially applicable for IAS management in the clinical setting.

Table 2 Prediction of IAS haemodynamics from real-world data

			Prediction from pre-IAS	
	Baseline	Measured	Constant V_T	Adjusted V_T
Q_P/Q_S	—	1.27	1.27	1.26
Q_P (L/min)	4.6	6.1	5.5	5.6
Q_S (L/min)	4.6	4.8	4.3	4.5
AP (mmHg)	96	97	91	(96 = Baseline)
P_{LA} (mmHg)	17.4	16.5	14.4	16.0
P_{RA} (mmHg)	9.0	10.6	9.6	11.4

Data are expressed as mean ± SD. AP, atrial pressure; IAS, interatrial shunt; P_{LA}, left atrial pressure; P_{RA}, right atrial pressure; Q_P, pulmonary flow; Q_S, systemic flow; V_T, total stressed blood volume.

The results of previous clinical trials[5–8] indicate that HFpEF is a good indication for IAS because rapid pulmonary congestion is a cardinal manifestation of HFpEF. In our simulation of HFpEF conditions, although baseline haemodynamics is relatively normal, volume loading or exercise significantly increases P_{LA} to above the critical level (*Figures 4* and *5*). IAS markedly attenuates the increase in P_{LA}. Interestingly, IAS does not mitigate Q_S during volume loading or exercise much. To elucidate the relationship among the severity of diastolic dysfunction in HFpEF, IAS size, and clinical benefit of IAS, we further simulated the exercise capacity after IAS placement at various levels of diastolic function and IAS sizes.

In reference to *Figure 6*, we altered diastolic function by changing the stiffness component (k) at three levels and conducted the same simulation study, as shown in *Figure 5*. An increase in k decreased CO and increased P_{LA}. We defined the exercise capacity by the peak exercise level when P_{LA} reached 28 mmHg.[21,24] As shown in *Figure 6*, in mild HFpEF, P_{LA} never reached the P_{LA} threshold when IAS size was over 5 mm. In moderate HFpEF, IAS size-dependently increased

DOI: 10.1002/ehf2.12935

FIGURE 6 The relationship between the exercise capacity and IAS diameter under various degrees of diastolic dysfunction in heart failure with preserved ejection fraction (HFpEF) in simulation study. We assumed left atrial pressure (P_{LA}) = 28 mmHg as the exercise capacity under IAS (A) and compared the exercise capacity among three levels of diastolic dysfunction in HFpEF condition (B). We altered diastolic function in HFpEF by changing k, which represents the ventricular stiffness and governs the curvilinearity of the cardiac output curve (mild = 1.23, moderate = 1.3, severe = 1.35). See text Area not definedMethods section for detail, regarding the definition of the intensity of exercise (0 to 1 W/kg). In mild HFpEF, P_{LA} does not exceed 28 mmHg by exercise under 1 W/kg when IAS size is over 5 mm. IAS strikingly increases exercise capacity, especially in moderate HFpEF. In severe HFpEF, IAS increases exercise capacity slightly. The solid line represents mild HFpEF, broken line represents moderate HFpEF, and dotted line represents severe HFpEF.

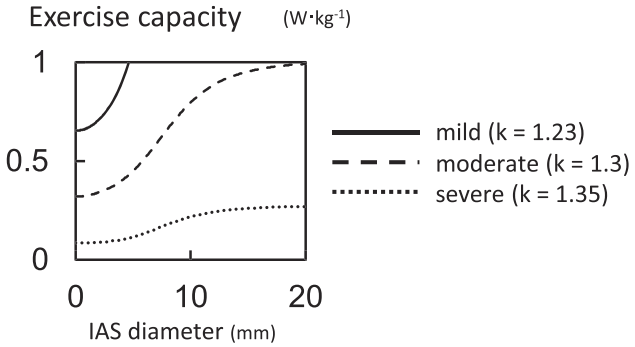

peak exercise. However, in severe HFpEF, the beneficial impact of IAS on exercise capacity was marginal because of high baseline P_{LA} (24.7 mmHg). These results indicate that IAS improves exercise capacity, especially in mild to moderate HFpEF conditions. Our simulation results are consistent with previous clinical trials.[5–8]

Regarding clinical feasibility, we need to consider IAS-induced increment of Q_P at rest. Increasing shear stress due to high Q_P increases the expression of proliferative genes and causes endothelial dysfunction, leading to pulmonary hypertension.[25] Therefore, shunt closure is recommended for atrial septal defect patients with $Q_P/Q_S > 1.5$.[26] As our proposed prediction method only addresses the acute effect, we have to consider various factors including age, severity of pulmonary hypertension, and right heart function for long-term risk stratification after IAS placement.

Our proposed framework could simulate the effect of IAS on haemodynamics in various cardiac conditions and perturbations (volume loading and exercise). Individualized quantitative prediction of the effect of IAS contributes to the optimization of IAS therapy.

Limitations

There are several limitations to this study. First, we conducted experiments using anaesthetised and open-chest dogs. Anaesthesia and surgical intervention change the cardiovascular system via the autonomic nervous system, blood volume loss, and artificial ventilation. We need to examine the feasibility of the framework under conscious condition to translate this method to clinical practice. Second, we mimicked IAS by creating a shunt flow using a centrifugal pump. Although mimicked IAS was anatomically different from clinical IAS, we adjusted the shunt flow rate according to the pressure gradient between left and right atria to simulate the different sizes of IAS. Third, to evaluate the impact of interatrial shunt flow on haemodynamics, we created an external shunt flow using a centrifugal pump. The pump-generated shunt flow in the animal model was unidirectional and constant and was different from the bidirectional and pulsatile IAS flow in patients in terms of fluid dynamics. This difference may affect the C_d (discharge coefficient) in equation 7. Because we used previously reported C_d, the accuracy of prediction of static haemodynamics by our framework should not have been affected. Nevertheless, further investigation may be needed to establish an appropriate mathematical model of IAS considering fluid dynamics to improve our IAS framework. Finally, we did not study the chronic effect of IAS, for example, ventricular remodelling. Although we speculate that the prediction in the acute phase may provide the beneficial effects in the chronic phase, further studies are needed to clarify the usability of the prediction for chronic IAS management.

Conclusions

In conclusion, we predicted the impact of IAS on haemodynamics reasonably well using the generalized circulatory equilibrium. Simulation study reveals how IAS attenuates the elevation of P_{LA} during volume loading conditions and exercise. Computational prediction of haemodynamics before the creation of an IAS would contribute to maximizing the benefit of IAS.

Acknowledgements

The authors thank Mr. Takuya Akashi and the staff of the Department of Cardiovascular Medicine, Kyushu University for technical support.

Conflict of interest

Nishikawa T., Uike K., Uemura K., Tohyama T., and Yoshida K. have nothing to declare. Saku K. and Kishi T. worked in a department endowed by Omron Healthcare Co. Saku K. received honoraria from Japan ABIOMED Inc. Sunagawa K. worked in a department endowed by Omron Healthcare Co.

and Actelion Pharmaceuticals Japan. Tsutsui H. received honoraria from Daiichi Sankyo, Inc., Otsuka Pharmaceutical Co., Ltd., Takeda Pharmaceutical Company Limited, Mitsubishi Tanabe Pharma Corporation, Boehringer Ingelheim Japan, Inc., Novartis Pharma K.K., Bayer Yakuhin, Ltd., Bristol-Myers Squibb KK, and Astellas Pharma Inc., and research funding from Omron Healthcare Co, Actelion Pharmaceuticals Japan, Daiichi Sankyo, Inc., and Astellas Pharma Inc.

Funding

This work was supported by Research and Development of Supportive Device Technology for Medicine Using ICT (18he1102003h0004), AMED-SENTAN; Development of Advanced Measurement and Analysis Systems (18hm0102041h0003), Grant-in-Aid for Early-Career Scientists (18K15893, 19K20690, and 19K17529) from the Japan Society for the Promotion of Science, the research grant from Omron Healthcare Co., and the Japan Foundation for Applied Enzymology (VBIC: Vascular Biology of Innovation).

Supporting information

Additional supporting information may be found online in the Supporting Information section at the end of the article.

Data S1. Supporting Information
Table S1. *Haemodynamics under mimicked interatrial shunting*
Table S2. *Values of model parameters that vary during exercise.*
Table S3. *Values of model parameters that are constant during exercise.*
Figure S1 *Supporting Information*

References

1. Lackland D. Heart disease and stroke statistics—2017 update: a report from the American Heart Association. *Circulation* 2017; **135**: e146–e603.
2. Fonarow GC. The Acute Decompensated Heart Failure National Registry (ADHERE): opportunities to improve care of patients hospitalized with acute decompensated heart failure. *Rev Cardiovasc Med* 2003; **4**: S21–S30.
3. Schiff GD, Fung S, Speroff T, McNutt RA. Decompensated heart failure: symptoms, patterns of onset, and contributing factors. *Am J Med* 2003; **114**: 625–630.
4. Goodlin SJ. Palliative care in congestive heart failure. *J Am Coll Cardiol* 2009; **54**: 386–396.
5. Hasenfub G, Hayward C, Burkhoff D, Silvestry FE, McKenzie S, Gustafsson F, Malek F, Van Der Heyden J, Lang I, Petrie MC, Cleland JGF, Leon M, Kaye DM. A transcatheter intracardiac shunt device for heart failure with preserved ejection fraction (REDUCE LAP-HF): a multicentre, open-label, single-arm, phase 1 trial. *Lancet* 2016; **387**: 1298–1304.
6. Feldman T, Mauri L, Kahwash R, Litwin S, Ricciardi MJ, van der Harst P, Penicka M, Fail PS, Kaye DM, Petrie MC, Basuray A, Hummel SL, Forde-McLean R, Nielsen CD, Lilly S, Massaro JM, Burkhoff D, Shah SJ, REDUCE LAP-HF I Investigators and Study Coordinators. Transcatheter interatrial shunt device for the treatment of heart failure with preserved ejection fraction (REDUCE LAP-HF I [reduce elevated left atrial pressure in patients with heart failure]): a phase 2, randomized, sham-controlled trial. *Circulation* 2018; **137**: 364–375.
7. Del Trigo M, Bergeron S, Bernier M, Amat-Santos IJ, Puri R, Campelo-Parada F, Altisent OA-J, Regueiro A, Eigler N, Rozenfeld E, Pibarot P, Abraham WT, Rodés-Cabau J. Unidirectional left-to-right interatrial shunting for treatment of patients with heart failure with reduced ejection fraction: a safety and proof-of-principle cohort study. *Lancet* 2016; **387**: 1290–1297.
8. Wessler J, Kaye D, Gustafsson F, Petrie MC, Hasenfuβ G, Lam CSP, Borlaug BA, Komtebedde J, Feldman T, Shah SJ, Burkhoff D, REDUCE-LAP-HF Trial Investigators and Advisors. Impact of baseline hemodynamics on the effects of a transcatheter interatrial shunt device in heart failure with preserved ejection fraction. *Circ Heart Fail* 2018; **11**: e004540.
9. Guyton AC. Determination of cardiac output by equating venous return curves with cardiac response curves. *Physiol Rev* 1955; **35**: 123–129.
10. Sunagawa K, Sagawa K, Maughan WL. Ventricular interaction with the loading system. *Ann Biomed Eng* 1984; **12**: 163–189.
11. Uemura K, Sugimachi M, Kawada T, Kamiya A, Jin Y, Kashihara K, Sunagawa K. A novel framework of circulatory equilibrium. *Am J Physiol Heart Circ Physiol* 2004; **286**: H2376–H2385.
12. Uemura K, Kawada T, Kamiya A, Aiba T, Hidaka I, Sunagawa K, Sugimachi M, Hidaka I, Sunagawa K, Sugimachi M. Prediction of circulatory equilibrium in response to changes in stressed blood volume. *Am J Physiol Heart Circ Physiol* 2005; **289**: H301–H307.
13. Sakamoto K, Saku K, Kishi T, Kakino T, Tanaka A, Sakamoto T, Ide T, Sunagawa K. Prediction of the impact of veno-arterial extracorporeal membrane oxygenation on hemodynamics. *Am J Physiol Heart Circ Physiol* 2015; **308**: H921–H930.
14. Kakino T, Saku K, Sakamoto T, Sakamoto K, Akashi T, Ikeda M, Ide T, Kishi T, Tsutsui H, Sunagawa K. Prediction of hemodynamics under left ventricular assist device. *Am J Physiol Heart Circ Physiol* 2017; **312**: H80–H88.
15. Shoukas AA. Pressure-flow and pressure-volume relations in the entire pulmonary vascular bed of the dog determined by two-port analysis. *Circ Res* 1975; **37**: 809–818.
16. Lee RW, Goldman S. Mechanism for decrease in cardiac output with atrial natriuretic peptide in dogs. *Am J Physiol* 1989; **256**: H760–H765.
17. Thomas JD, Weyman AE. Fluid dynamics model of mitral valve flow: description with in vitro validation. *J Am Coll Cardiol* 1989; **13**: 221–233.
18. Trudnowski RJ, Rico RC. Specific gravity of blood and plasma at 4 and 37°C. *Clin Chem* 1974; **20**: 615–616.
19. Wolsk E, Kaye D, Komtebedde J, Shah SJ, Borlaug BA, Burkhoff D, Kitzman DW, Lam CSP, van Veldhuisen DJ, Ponikowski P, Petrie MC, Hassager C, Møller JE, Gustafsson F. Central and peripheral determinants of exercise capacity in heart failure patients with preserved ejection fraction. *JACC Heart Fail* 2019; **7**: 321–332.

20. Miller WL, Mullan BP. Volume overload profiles in patients with preserved and reduced ejection fraction chronic heart failure: are there differences? A pilot study. *JACC Heart Fail* 2016; **4**: 453–459.
21. Maeder MT, Thompson BR, Brunner-La Rocca HP, Kaye DM. Hemodynamic basis of exercise limitation in patients with heart failure and normal ejection fraction. *J Am Coll Cardiol* 2010; **56**: 855–863.
22. Kaye D, Shah SJ, Borlaug BA, Gustafsson F, Komtebedde J, Kubo S, Magnin C, Maurer MS, Feldman T, Burkhoff D. Effects of an interatrial shunt on rest and exercise hemodynamics: results of computer simulation in heart failure. *J Card Fail* 2014; **20**: 212–221.
23. Sakamoto T, Kakino T, Sakamoto K, Tobushi T, Tanaka A, Saku K, Hosokawa K, Onitsuka K, Murayama Y, Tsutsumi T, Ide T, Sunagawa K, Hosokawa K, Onitsuka K, Murayama Y, Tsutsumi T, Ide T. Changes in vascular properties, not ventricular properties, predominantly contribute to baroreflex regulation of arterial pressure. *Am J Physiol Heart Circ Physiol* 2015; **308**: H49–H58.
24. Borlaug BA, Melenovsky V, Koepp KE. Inhaled sodium nitrite improves rest and exercise hemodynamics in heart failure with preserved ejection fraction. *Circ Res* 2016; **119**: 880–886.
25. Hemnes AR, Humbert M. Pathobiology of pulmonary arterial hypertension: understanding the roads less travelled. *Eur Respir Rev* 2017; **26**: 170093.
26. Stout KK, Daniels CJ, Aboulhosn JA, Bozkurt B, Broberg CS, Colman JM, Crumb SR, Dearani JA, Fuller S, Gurvitz M, Khairy P, Landzberg MJ, Saidi A, Valente AM, Van Hare GF. 2018 AHA/ACC guideline for the management of adults with congenital heart disease: a report of the American College of Cardiology/American Heart Association Task Force on Clinical Practice Guidelines. *Circulation* 2019; **139**: e698–e800.